Development of vardenafil hydrochloride-loaded silica nanoparticles with enhanced transdermal delivery

Hussein O. AMMAR[1] ID , Mina Ibrahim TADROS[2] ID , Nahla M. SALAMA[1] ID , Amira Mohsen GHONEIM[1*] ID

[1] Department of Pharmaceutics and Pharmaceutical Technology, Faculty of Pharmacy, Future University in Egypt (FUE), New Cairo, Egypt.
[2] Department of Pharmaceutics and Industrial Pharmacy, Faculty of Pharmacy, Cairo University, Cairo, Egypt.
 *Corresponding Author A.G.. E-mail: amohsen@fue.edu.eg Tel. +20 1223124998.

ABSTRACT: The aim of the present study was to develop a promising silica nanoparticle system to enhance the transdermal delivery of vardenafil hydrochloride (VRD) for treatment of erectile dysfunction. VRD-loaded silica nanoparticles were prepared using chitosan, polyethylene glycol and tetraethyl orthosilicate. The systems were monitored for vesicle size, zeta potential, drug entrapment efficiency, permeation of the drug after 0.5 hour ($Q_{0.5h}$) and after 12 hours (Q_{12h}). The utmost achieved system (VRD-SNP5) was histopathologically examined for skin irritation, and evaluated via confocal laser scanning microscopy (CLSM). VRD-SNP5 system and an oral aqueous drug dispersion were used to determine VRD pharmacokinetic parameters using physiologically based pharmacokinetic (PBPK) modeling. The VRD-SNP5 system comprised spherical vesicles (440.50 nm) possessing high zeta potential (26.00 mV), promising EE percent (71.5%), low $Q_{0.5h}$ (39.5±2.6%), and high Q_{12h} (91.5±4.5%). It exhibited modest histopathologic alterations in rat skin after a 12-hour leave-on period. CLSM revealed deep drug penetration via rat skin. Following the transdermal application of the VRD-SNP5 system, PBPK modeling proposed the achievement of lower C_{max} values, delayed T_{max} estimates, and higher AUC_{0-24h} folds in adults (3 folds) and geriatrics (1.65 folds). It could be concluded that silica nanoparticles could represent a potential transdermal delivery system for VRD.

KEYWORDS: Vardenafil-1; silica-2; nanoparticles-3; transdermal-4; pharmacokinetic-5.

1. INTRODUCTION

Erectile dysfunction (ED) is the inability to initiate or maintain a firm erection of the penis during sexual activity [1]. ED is a common illness associated with ageing that has a significant impact on men's and their spouses' quality of life. According to recent studies, vascular disorders are the most prevalent cause of ED in nearly 90% of men over the age of 40 [2]. The severity of ED is linked to vascular risk factors that are accompanied by endothelial dysfunction, where the vascular endothelium plays a crucial role in maintaining corpora cavernosa vascular homeostasis [3]. High blood pressure, dyslipidemia, atherosclerosis, Parkinson's disease, coronary artery disease, smoking, and diabetes mellitus are among these risk factors [4]. Damage to the nerves involved in erections, particularly following prostate surgery, is another cause of ED [5].

Phosphodiesterase type 5 (PDE5) inhibitors have demonstrated efficacy for treatment of ED. Oral PDE5 inhibitors are now one of the most often prescribed medicines for individuals with ED [6]. This class of medicines has a number of advantages, including simplicity of administration and cheap prices.VRD is extremely beneficial in individuals with premature ejaculation, even if they do not have ED symptoms, according to primary research [7]. Men were randomized to receive VRD (10 or 20 mg) or placebo in clinical studies. Without regard to age, etiology, or the existence of post-prostatectomy ED, there was a substantial improvement in ED in VRD patients [8]. However, VRD suffers from low bioavailability, due to hepatic first-pass metabolism [9].

Because of its unique features, such as a hydrophilic surface that promotes prolonged circulation after IV administration, ease of synthesis, and low cost of manufacture, silica nanoparticles (SNPs) have gained a lot of attention [10, 11]. SNPs are being developed for a variety of medical applications, including diagnosis and therapy [12, 13], biomarker probes for optical imaging [14] controlled release medication delivery, and

gene transfection carriers [11]. Skin cancer [15-17], transdermal medication delivery [18], and gene delivery [19] are only a few of the uses for such medicinal nanoparticles. They can act as a carrier for low-solubility medicines, potentially improving drug safety, stability, and efficacy.

The pharmacokinetic characteristics of VRD entrapped in SNP5 were predicted using physiologically based pharmacokinetic modelling (PBPK). Simcyp® Simulator was the program utilized (V17.1; Certara, Sheffield, UK). Drug Absorption (Skin): MechDermA Model was the model used. PBPK models are based on the body's anatomical and physiological structure, as well as biochemistry to some extent. Typically, they are multi-compartment models with compartments corresponding to designated organs or tissues and linkages corresponding to blood or lymph flows (more rarely to diffusions). It is possible to write a system of differential equations for the amount of a drug in every compartment, with the parameters representing blood flows, pulmonary ventilation rate, organ volumes, which could be found in scientific publications. Indeed, their representation of the body is simplified, and a balance between complexity and simplicity of the body systems must be achieved [20].

VRD-loaded silica nanoparticles were developed using chitosan, polyethylene glycol and tetraethyl orthosilicate. The systems were subjected to *in vitro* and *ex vivo* evaluations. The pharmacokinetics of the best achieved system were estimated using physiologically based pharmacokinetic modeling.

2. RESULTS AND DISCUSSION

2.1. Characterization of VRD-loaded SNPs

2.1.1. *Evaluation of vesicle size, polydispersity index and zeta potential*

The results of the *in vitro* characterization studies of VRD-SNPs are listed in Table 1. VRD-SNP1 had the smallest size (360.8 nm), followed by VRD-SNP2 (425.7 nm) and VRD-SNP3 (484.9 nm). The results demonstrated a clear relationship between chitosan concentration and vesicle size. Bangun et al. [28] reported similar findings, revealing that the smallest size was produced from the lowest chitosan concentration. Compared to VRD-SNP2, VRD-SNP4 and VRD-SNP5 showed no significant difference ($P > 0.05$) in particle size. It could be inferred that increasing TEOS concentration, at a fixed chitosan concentration, did not affect the particle size.

Table 1. The composition and the physicochemical properties of the investigated vardenafil hydrochloride-loaded silica nanoparticles; in comparison to drug aqueous dispersion (mean ± S.D., n = 3)

Systems	Composition		Physicochemical properties					
	Chitosan (g)	TEOS (g)	Particle Size (nm)	PDI	EE (%)	Zeta (mV)	$Q_{0.5h}$ (%)	Q_{12h} (%)
Drug dispersion							8.2±1.4	16.2±3.8
VRD-SNP1	0.05	0.2	360.8±18.0	0.40	55.5± 2.4	25.0±1.2	15.0±0.7	60.8±3.0
VRD-SNP2	0.10	0.2	425.7±21.2	0.47	62.7± 3.7	23.0±1.1	20.0±1.0	80.0±4.0
VRD-SNP3	0.15	0.2	484.9±24.2	0.55	73.6± 0.8	35.0±1.7	12.0±0.6	30.8±1.6
VRD-SNP4	0.10	0.1	430.6±21.5	0.39	70.5± 3.0	20.0±1.2	10.5±0.3	42.4±2.1
VRD-SNP5	0.10	0.4	440.5±22.0	0.43	71.5± 1.6	26.0±1.3	39.5±2.6	91.5±4.5

*All systems contained Vardenafil hydrochloride, 20 mg and PEG, 0.1 g.

The positive charge of the zeta potential, on the other hand, is consistent with earlier research [29, 30] and could be related to the primary amino group in the structure of chitosan. High zeta potential values

would ensure high physical stability. The prepared VRD-SNPs had a relatively acceptable vesicle size distribution with PDI values ranging from 0.39 to 0.55.
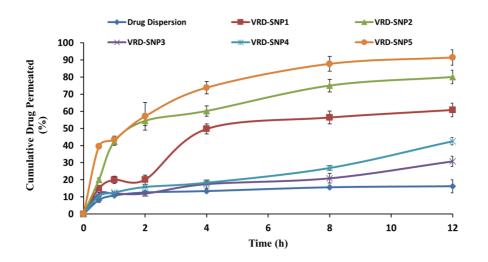
2.1.2. Determination of VRD entrapment efficiency

A direct correlation was observed between VRD EE% and chitosan concentration (Table 1). These findings were in line with those reported by Nagarajan et al. [31], who found that the drug EE% was increased with the increase in chitosan concentration up to 0.5%. Compared to VRD-SNP2, VRD-SNP4 and VRD-SNP5 showed no significant difference ($P>0.05$) in VRD EE%.

2.1.3. Ex vivo drug permeation study for VRD-loaded SNPs

The *ex vivo* VRD permeation profiles of VRD-SNPs, compared to VRD aqueous dispersion, are shown in Figure 1. It is clear that VRD-SNP2 has the highest percent of drug permeated after 0.5 and 12 hours ($Q_{0.5\%}$, $Q_{12\%}$), suggesting its superiority over VRD-SNP1 and VRD-SNP3. As a result, VRD-SNP2 was chosen for further characterization studies. The amount of TEOS in VRD-SNP2 was halved (VRD-SNP4) and doubled (VRD-SNP5). The values of $Q_{0.5\%}$ and $Q_{12\%}$ for VRD-SNP5 were significantly higher ($P<0.05$) than other VRD-SNPs systems. It could be inferred that increasing TEOS concentration, at a fixed chitosan concentration, had a significant effect on $Q_{0.5\%}$ and $Q_{12\%}$. $Q_{0.5\%}$ values between 30 – 40% are needed to initiate drug response while high $Q_{12\%}$ values are required to maintain this response for a prolonged period.
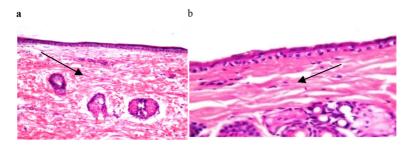
Based on the aforementioned findings, VRD-SNP5 was chosen for further investigations since it had promising particle size (440.5 nm), satisfying zeta potential (26.0 mV), high VRD EE% (71.5%), suitable $Q_{0.5\%}$ (39.5%) and high $Q_{12\%}$ (91.5%).

Figure 1. *Ex vivo* permeation of VRD from SNPs, in comparison to an aqueous VRD dispersion (mean± SD, n = 3)
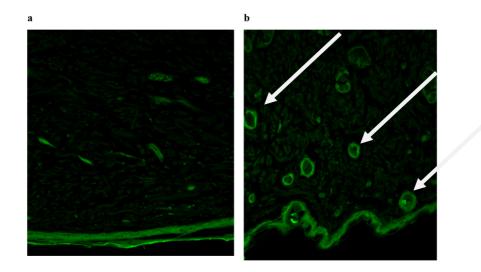
2.2. Histopathology of VRD-SNP5

When comparing VRD-SNP5 skin sections with the control skin samples, light microscopic examination revealed no histopathologic changes in the epidermis or the dermis (Figure 2). The control skin sample revealed normal skin architecture, including well-defined epidermis, dermis, and subcutaneous tissue, as well as sebaceous glands and hair follicles [24]. In a parallel line, no symptoms of skin irritation such as erythema or edema were noticed following exposure to the optimized VRD-SNP5. No histopathologic alterations were found in the skin samples, indicating that VRD-SNP5 shows good biocompatibility, a relatively acceptable safety profile and is not expected to cause irritation upon application to skin [32].
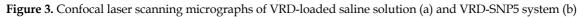
Figure 2. Histopathologic micrographs of hematoxylin and eosin-stained rat skin samples treated with (a) normal saline solution [24] and (b) VRD-SNP5 system

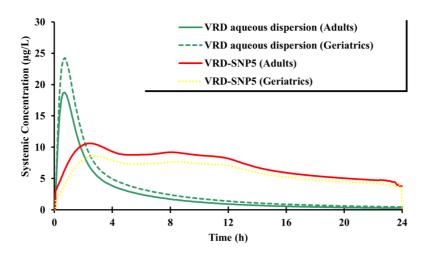### 2.3. Confocal laser scanning microscopy of VRD-SNP5

The CLSM investigation was carried out to confirm the potential of VRD-SNP5 to promote VRD skin permeation, relative to VRD-loaded saline solution. The hair follicles showed high fluorescence intensity upon application of VRD-SNP5 (Figure 3). It could be inferred that the follicular pathway plays the most important role in SNP transdermal penetration [33-35]. Because the hair follicles are surrounded by a thick network of blood capillaries, molecules passing through them are able to reach the tissue surrounding the follicle and enter the bloodstream, bypassing the stratum corneum barrier [36, 37].

Figure 3. Confocal laser scanning micrographs of VRD-loaded saline solution (a) and VRD-SNP5 system (b)

2.4. PBPK Modeling

The predicted VRD plasma concentration versus time curves following the transdermal application of VRD-SNP5 system and oral VRD aqueous dispersion in adults and geriatrics are depicted in Figure 4. The pharmacokinetic parameters are shown in Table 2. Following transdermal application of VRD-SNP5, the mean C_{max} valueswere 11.10 µg/L and 9.18 µg/L for adults and geriatric populations, respectively. These C_{max} values were lower than their corresponding ones after administration of VRD oral dispersion. On the other hand, T_{max} and AUC_{0-24h} values were higher after transdermal application, compared to the oral dispersion. These results reveal that after transdermal application of VRD-SNP5, the drug was released in a controlled, prolonged pattern, with enhanced bioavailability.

Figure 4. Physiologically based pharmacokinetic model simulated vardenafil hydrochloride plasma concentration–time curves following transdermal application of VRD-SNP5 and an oral drug dispersion, at 20 mg doses, in adults and geriatrics.

Table 2. Pharmacokinetics parameters of vardenafil hydrochloride after transdermal application of VRD-SNP5 System and an oral drug dispersion, at 20 mg doses, in adults and geriatrics (n = 100)

Treatment dose of 20 mg	Population	T_{max} (h)*	C_{max} (µg/L)	AUC_{0-24h} (µg/L.h)
Oral dispersion	Adult	0.7 (0.5-1.2)	18.7 3± 6.54	59.3 ± 10.9
	Geriatric	0.72 (0.4-1.1)	24.27 ± 11.75	79.33 ± 43.82
VRD-SNP5	Adult	3.15 (1.5-7.5)	11.10 ± 4.19	171.72 ± 62.71
	Geriatric	3.35 (3.7-24)	9.18 ± 4.10	144.69 ± 44.73

*Median (range)

As for the geriatric population, there was a noticeable change in the pharmacokinetic parameters after both oral and transdermal application. After oral administration of VRD, C_{max} and AUC_{0-24h} values were greater, compared to the adult population. This could be explained by the reduction of glomerular filtration rate and hepatic clearance which occurs in the elderly [24]. On the contrary, these two values were lower after transdermal application in the geriatric population. This reduction in the bioavailability of the drug could be attributed to the skin physiological changes, in terms of thickness of skin layers, the water content and the density of the hair follicle, after ageing.

3. CONCLUSION

VRD-loaded SNPs were successfully developed by the dispersion approach using chitosan, TEOS and PEG. Of the investigated systems, VRD-SNP5 had promising particle size (440.5 nm), satisfying zeta potential (26.0 mV), high VRD EE% (71.5%), suitable $Q_{0.5\%}$ (39.5%) and high $Q_{12\%}$ (91.5%). Furthermore, it showed no signs of histopathologic changes in rat skin and had a promising drug permeation potential through skin layers. PBPK modeling proved the superiority of VRD-SNP5 over the aqueous dispersion, in terms of drug bioavailability. Further clinical studies are needed to confirm the capability of this drug delivery system in treating patients suffering from erectile dysfunction.

4. MATERIALS AND METHODS

4.1. Materials

Vardenafil hydrochloride was kindly supplied by Marcyrl Pharmaceutical Industries (Cairo, Egypt). Sodium chloride, di-sodium hydrogen phosphate, potassium chloride, sodium di-hydrogen phosphate, acetic acid, were purchased from El-Nasr Pharmaceutical Chemicals Co. (Cairo, Egypt). Tetraethyl orthosilicate (TEOS) was obtained from Merck KGaA Darmstadt, Germany. L-α-phosphatidylcholine (PC, Type IV-S), ethanol (HPLC grade), Chitosan (degree of deacetylation; 90% - Molecular weight; 161 kDa), acetonitrile (HPLC grade), Polyethylene Glycol 400 (PEG 400) and Rhodamine B were purchased from Sigma-Aldrich Chemical Co. (St. Louis, MO).

4.2. Formulation of VRD-loaded SNPs

The dispersion approach was used to prepare VRD-loaded SNPs (VRD-SNP) [17]. For the development of single-dose system, VRD (20 mg) was dissolved in 0.05 M phosphate buffer saline (pH 7, 1 mL). PEG (0.1 mL), chitosan (0.05, 0.1, and 0.15 g), and hydrolyzed TEOS (0.2 g) were incorporated. The mixture was homogenized at 5000 rpm (Heidolph Silent Crusher M, Schwabach, Germany) till a firm gel is formed. It is worth to note that the hydrolyzed TEOS was made by combining water, glacial acetic acid, and TEOS in a 1:1:0.25 ratio using the sol-gel process [21]. When a clear solution is created due to complete hydrolysis of TEOS by acetic acid as a catalyst, it was incubated for 1 hour.

4.3. Characterization of VRD-loaded SNPs

4.3.1. Evaluation of particle size, polydispersity index and zeta potential

In a flask, one gram of each formulation was diluted (to 100 mL) and gently mixed with distilled water. The particle size, zeta potential, and polydispersity index were measured using photon correlation spectroscopy, which analyses the variation in light scattering caused by the brownian motion of the droplets as a function of time. Light scattering was measured at a 90° angle at 25°C with Zetasizer (Malvern Zetasizer Nanoseries, Worcestershire, UK) [22].

4.3.2. Determination of VRD entrapment efficiency

Entrapment efficiency (EE) of VRD was determined by diluting VRD-SNPs with phosphate buffered saline, followed by ultracentrifugation at 15000 rpm for 1 h at 4 °C (1 h;4°C) (HeraeusMegafuge® 1.0 R; Hanau, Germany). The supernatant was separated, and the absorbance at 250 nm was determined spectrophotometrically. The following equation [23] was used to calculate the EE value:

$$\% \text{ Entrapment Efficiency} = \frac{\{VRD\}total - \{VRD\}supernatant}{\{VRD\}total} \times 100$$

Where, $\{VRD\}_{total}$ is the amount of loaded drug in the system and $\{VRD\}_{supernatant}$ is the amount of drug measured in the supernatant.

4.3.3. Ex vivo drug permeation study

The *ex vivo* drug permeation studies were approved by the Animal Ethics Committee of the Faculty of Pharmacy, Future University in Egypt (FUE); approval No REC-FPSPI-7/47. An overdose of sodium thiopental was used to sacrifice the rats. The hair was shaved away with an electric shaver. Following, the full-thickness skin was retrieved and examined for scratches, bites, or other anomalies before the subcutaneous fat was gently removed without harming the epidermis. Before the experiment, the skin was put in a phosphate buffered-saline solution for 10 minutes. The skin was kept at -20°C while not in use and utilized within 3 days of harvest. The skin was thawed to room temperature before being equilibrated in phosphate buffered-saline (pH 7.4) for 1 hour before conducting the drug permeation studies using Franz diffusion cells (Hanson research, Vision® Microette™ automated diffusion test system, Chatsworth, CA).

The skin sample (1.76 cm²) was mounted between the donor and receptor chamber of each cell so that the epidermal surface is facing upwards. The receptor chamber was loaded with phosphate buffer saline (pH 7.4) and was kept at a stirring rate of 600 rpm at 32°C ± 0.5°C. The autosampler was adjusted to collect aliquots at 0.5, 1, 2, 4, 8, and 12 hours and the receptor chamber was replenished with fresh medium to ensure sink conditions. The samples were analyzed using a validated HPLC assay [24]. For each system, the permeated amount of VRD was plotted against time. The findings were compared to those of VRD aqueous dispersion.

4.3.4. HPLC system

Samples were tested using HPLC to determine VRD concentration. A chromatographic system (Shimadzu Tokyo, Japan) with a Shimadzu LC-10 AD VP pump, DGU-12A degasser, and SCL-10A VP system controller comprised the system. At 250 nm, samples were injected using a Spectra System Auto Sampler AS4000 at 1 ml/min flow rate. The Waters C18 column (10 μm particle diameter 125A, Bondpak, 4.6 x 250 mm) was employed. In an isocratic elution mode, a mobile phase of 70 % phosphate buffered-saline (pH 7.4) and 30% acetonitrile was utilized [24].

4.4. Histopathology of selected VRD-loaded SNPs

Histopathologic studies were conducted to determine the safety of the best achieved system. A sample of VRD-SNPs was placed onto the skin of rats. After 12 hours, the animal was sacrificed, and post-mortem skin samples from rats were taken and fixed in 10% formalin saline for 24 hours. Dehydration was achieved using serial dilutions of alcohol (methyl-, ethyl-, and absolute ethyl-alcohol) after washing with water. Specimens were cleaned in xylene before being embedded in paraffin in a hot air oven for 24 hours at 56 °C. Paraffin beeswax tissue blocks with a thickness of 4 microns were produced using a sledge microtome. Tissue slices were taken on glass slides, deparaffinized, and stained with hematoxylin and eosin for routine as well as alizarin red for inspection via the microscope. The obtained tissue sections were collected on glass slides, deparaffinized, stained by hematoxylin and eosin stain and finally examined through the light electric microscope and compared with a control skin sample treated with normal saline [25].

4.5. Confocal laser scanning microscopy of VRD-loaded SNPs

A fluorescent dye, rhodamine B, was added to the best achieved VRD-SNPs at a concentration of 0.1 % (w/v) for conducting confocal laser scanning microscopy (CLSM). As a control sample, the dye was mixed, at a similar concentration, with 0.9 % sodium chloride solution containing VRD. The e*x vivo* drug permeation studies were conducted as outlined earlier. After 12 hours, the skin samples (test and control) were removed from the diffusion cells, washed with distilled water, and kept in 10% (v/v) formalin in phosphate buffered-saline for 24 hours (pH 7.4). Probe penetration was evaluated when the skin was vertically cross-sectioned into 0.5 mm² sections. The skin's whole thickness was optically scanned. The 10 objective lens system of an inverted Zeiss LSM 510 META microscope (Carl Zeiss, Jena, Germany) coupled with a He–Ne laser was used for visualization. The wavelengths utilized for excitation and emission were 562 nm and 587 nm, respectively [26].

4.6. PBPK modeling

The input data required for building the PBPK model for VRD was reported in our previous work [24]. Preliminary verification of the PBPK model for VRD has been successfully achieved, wherea comparison between the predicted and observed data by Stark et al [27], showed that mean predicted/observed ratios for T_{max}, C_{max}, and AUC_{0-24h} were 1.06, 0.98 and 0.82, respectively [24]. In the current work, pharmacokinetic modeling was carried out to compare the pharmacokinetic parameters (T_{max}, C_{max}, and AUC_{0-24h}) of VRD from oral aqueous dispersion and transdermal VRD-SNPs in both adults and geriatric populations.

4.7. Statistical analysis

All the results were analyzed by applying two-way analysis of variance (ANOVA) followed by post-hoc test using SPSS® software (IBM 20, USA).

Author contributions: Concept – H.M., M.T., N.S., A.G.; Design – H.M., M.T., N.S., A.G.; Supervision – H.M., M.T., N.S., A.G.; Resources – H.M., M.T., N.S., A.G.; Materials – H.M., M.T., N.S., A.G.; Data Collection and/or Processing – H.M., M.T., N.S., A.G.; Analysis and/or Interpretation – H.M., M.T., N.S., A.G.; Literature Search – H.M., M.T., N.S., A.G.; Writing – H.M., M.T., N.S., A.G.; Critical Reviews – H.M., M.T., N.S., A.G.

Conflict of interest statement: The authors declared no conflict of interest" in the manuscript.

Ethics Commitee approval: The *ex vivo* protocol was approved by Animal Ethics Committee at the Faculty of Pharmacy-Future University in Egypt, Cairo, Egypt (Approval number: REC-FPSPI-7/47).

REFERENCES

[1] Voznesensky M, Annam K, Kreder KJ. Understanding and managing erectile dysfunction in patients treated for cancer. J Oncol Pract. 2016;12:297-304. [CrossRef]

[2] Dean RC, Lue DF. Physiology of penile erection and pathophysiology of erectile dysfunction. Urol Clin North Am. 2005;32:379-395. [CrossRef]

[3] Maas R, Schwedhelm E, Albsmeier J, Boger RH. The pathophysiology of erectile dysfunction related to endothelial dysfunction and mediators of vascular function. Vasc Med. 2002;7:213-225. [CrossRef]

[4] Andersson KE, Wagner G. Physiology of penile erection. Physiol Rev. 1996;75:191-236. [CrossRef]

[5] Krause ND, Duckles SP, Pelligrino DA. Influence of sex steroid hormones on cerebrovascular function. J Appl Physiol. 2006;101:1252-1261. [CrossRef]

[6] Andersson KE, de Groat WC, McVary KT, Lue TF, Maggi M, Roehrborn GC. Tadalafil for the treatment of lower urinary tract symptoms secondary to benign prostatic hyperplasia: pathophysiology and mechanism(s) of action. Neurourol Urodyn. 2011;30:292-301. [CrossRef]

[7] Jannini EA, McMahon C, Chen J. The controversial role of phosphodiesterase type 5 inhibitors in the treatment of premature ejaculation. J Sex Med. 2011;8:2135-2143. [CrossRef]

[8] Song SH, Kim DS, Shim SH, Lim JJ, Yang SC. Usage and perceptions of phosphodiesterase type 5 inhibitors among the male partners of infertile couples. Clin Exp Reprod Med. 2016;43:26-30. [CrossRef]

[9] Gupta M, Kovar A, Meibohm B. The clinical pharmacokinetics of phosphodiesterase-5 inhibitors for erectile dysfunction. J Clin Pharmacol. 2005;45:987-1003. [CrossRef]

[10] Barbe C, Bartlett J, Kong LG, Finnie K, Lin HQ, Larkin M. Silica particles: a novel drug-delivery system. Adv Mater. 2004;16:1959–1966. [CrossRef]

[11] Slowing II, Vivero-Escoto JL, Wu CW, Lin VSY. Mesoporous silica nanoparticles as controlled release drug delivery and gene transfection carriers. Adv Drug Deliv Rev. 2008;60:1278–1288. [CrossRef]

[12] Tang L, Cheng J. Nonporous silica nanoparticles for nanomedicine application. Nano Today.2013;8:290–312. [CrossRef]

[13] Tang F, Li L, Chen D. Mesoporous silica nanoparticles: synthesis, biocompatibility and drug delivery. Adv Mater. 2012;24:1504–1534. [CrossRef]

[14] Lee CH, Cheng SH, Wang YJ, Chen YC, Chen NT, Souris J. Near-infrared mesoporous silica nanoparticles for optical imaging: characterization and in vivo biodistribution. Adv Funct Mater. 2009;19:215–212. [CrossRef]

[15] Benezra M, Penate-Medina O, Zanzonico PB, Schaer D, Ow H, Burns A. Multimodal silica nanoparticles are effective cancer targeted probes in a model of human melanoma. J Clin Invest. 2011;121:2768–2780. [CrossRef]

[16] DeLouise LA. Applications of nanotechnology in dermatology. J Invest Dermatol. 2012;132:964–9675. [CrossRef]

[17] Scodeller P, Catalano PN, Salguero N, Duran H, Wolosiuk A, Soler-Illia GJAA. Hyaluronan degrading silica nanoparticles for skin cancer therapy. Nanoscale. 2013;5:9690–9698. [CrossRef]

[18] Prausnitz MR, Elias PM, Franz TJ, Schmuth M, Tsai JC, Menon GK. Skin barrier and transdermal drug delivery. In: Bolognia J, Jorizzo JL, Schaffer JV, editors. Dermatology. Philadelphia, PA: Elsevier Saunders; 2012. p. 2065–2673.

[19] Bharali DJ, Klejbor I, Stachowiak EK, Dutta P, Roy I, Kaur N. Organically modified silica nanoparticles: a nonviral vector for in vivo gene delivery and expression in the brain. Proc Natl Acad Sci.2005;102:11539–11544. [CrossRef]

[20] Jones H, Rowland-Yeo K. Basic concepts in physiologically based pharmacokinetic modeling in drug discovery and development. CPT Pharmacometrics Syst Pharmacol. 2013 Aug 14;2(8):e63. [CrossRef]

[21] Friedman AJ, Han G, Navati MS, Chacko M, Gunther L, Alfieri A, Friedman JM. Sustained release nitric oxide releasing nanoparticles: Characterization of a novel delivery platform based on nitrite containing hydrogel/glass composites. Nitric Oxide. 2008;19:12-20. [CrossRef]

[22] Shahin HI, Vinjamuri BP, Mahmoud AA, Shamma RN, Mansour SM, Ammar HO, Ghorab MM, Chougule MB, Chablani L. Design and evaluation of novel inhalable sildenafil citrate spray-dried microparticles for pulmonary arterial hypertension. J Control Release. 2019;302:126–139. [CrossRef]

[23] Ammar HO, Ghorab MM, Mostafa DM, Ibrahim ES. Folic acid loaded lipid nanocarriers with promoted skin antiaging and antioxidant efficacy. J Drug Deliv Sci Technol. 2015;31:72–82. [CrossRef]

[24] Ammar HO, Tadros MI, Salama NM, Ghoneim AM. Ethosome-Derived Invasomes as a Potential Transdermal Delivery System for Vardenafil Hydrochloride: Development, Optimization and Application of Physiologically Based Pharmacokinetic Modeling in Adults and Geriatrics. Int J Nanomedicine. 2020;6:5671-5685. [CrossRef]

[25] Elfer KN, Sholl AB, Wang M, Tulman DB, Mandava SH, Lee BR, Brown JQ. DRAQ5 and Eosin ('D&E') as an analog to hematoxylin and eosin for rapid fluorescence histology of fresh tissues. PLoS One. 2016;11:e0165530. [CrossRef]

[26] Schatzlein A, Cevc G. Non-uniform cellular packing of the stratum corneum and permeability barrier function of intact skin: a high-resolution confocal laser scanning microscopy study using highly deformable vesicles (Transfersomes). Br J Dermatol. 1999;4:583–592. [CrossRef]

[27] Stark S, Sachse R, Liedl T, Hensen J, Rohde G, Wensing G, Horstmann R, Schrott KM. Vardenafil increases penile rigidity and tumescence in men with erectile dysfunction after a single oral dose. Eur Urol. 2001;40(2):181–188. [CrossRef]

[28] Bangun H, Tandiono S, Arianto A. Preparation and evaluation of chitosan-tripolyphosphate nanoparticles dispersion as an antibacterial agent. J Appl Pharm Sci. 2018;8:147-156. [CrossRef]

[29] Febriana CI, Indah N, Samsuridjal D, Mohamad S, Arief BW, Tomohiko Y. Preparation, characterization, and evaluation of chitosan-based nanoparticles as CpG ODN carriers. Biotechnol Equip.2019;33:390-396. [CrossRef]

[30] Asasutjarit R, Chayanid ST, Nardauma T, Sirijit P. Effect of formulation compositions on particle size and zeta potential of diclofenac sodium-loaded chitosan nanoparticles. Int J Pharmacol Pharm Sci. 2013;7:568-5670. [CrossRef]

[31] Nagarajan E, Shanmugasundaram P, Ravichandiran V, Vijayalakshmi A, Senthilnathan B, Masilamani K. Development and evaluation of chitosan based polymeric nanoparticles of an antiulcer drug lansoprazole. J Appl Pharm Sci. 2015;5:20-25. [CrossRef]

[32] Albash R, Abdelbary AA, Refai H, El-Nabarawi MA. Use of transethosomes for enhancing the transdermal delivery of Olmesartan medoxomil: in vitro, ex vivo, and in vivo evaluation. Int J Nanomedicine.2019;14:1953–1968. [CrossRef]

[33] Alvarez-Roman R, Naik A, Kalia YN, Guy RH, Fessi H. Skin penetration and distribution of polymeric nanoparticles. J Control Release. 2004;99:53-62. [CrossRef]

[34] Knorr F, Lademann J, Patzelt A, Sterry W, Blume-Peytavi U, Vogt A. Follicular transport route – research progress and future perspectives. Eur J Pharm Biopharm.2009;71:173-180. [CrossRef]

[35] Lademann J, Richter H, Teichmann A, Otberg N, Blume-Peytavi U, Luengo J, Weiß B, Schaefer UF, Lehr CM, Wepf R, Sterry W. Nanoparticle an efficient carrier for drug delivery into the hair follicles. Eur J Pharm Biopharm. 2007;66:159-164. [CrossRef]

[36] Otberg N, Teichmann A, Rasuljev U, Sinkgraven R, Sterry W, Lademann J. Follicular penetration of topically applied caffeine via a shampoo formulation. Skin Pharmacol Physiol. 2007;20:195-198. [CrossRef]

[37] Wosicka H, Cal K. Targeting to the hair follicles: current status and potential. J Dermatol Sci. 2010;57:83-89. [CrossRef]